

A Novel Technique for Smoothing Wind Farm Output Power Intermittency

Arfan M. Salih Hassan^{1*}, Dlzar Al Kez²

^{1*} Kalar Technical College, Sulaimani Technical Institute, Sulaimaniyah, Iraq (corresponding author)

² School of Mechanical and Aerospace Engineering, Queen's University Belfast, Belfast, UK

erfansolayee@gmail.com; dalkez01@qub.ac.uk

ABSTRACT

In recent decades, climate change has evolved from a hypothetical threat to the earth and its inhabitants to a terrifying fact. It is occurring simultaneously that the price of oil and natural gas continues to rise, endangering the national economy and global security. As a result, seeking alternative renewable energy sources has become a pressing necessity. However, one of the main issues with wind and solar energy is that it is variable and intermittent, resulting in erroneous output power projections. To address this issue, the main objective of this paper is to present and analyze a new strategy for reducing the output power intermittency of distributed wind farms. Instead of aggregating all wind turbines in one location, the proposed approach distributes a large number of wind turbines throughout diverse geographical locations with significant wind potential energy. The total output power generation from all wind turbines is then aggregated through a single control system, which injects the power into the grid in a manner similar to a virtual power plant. Later, the analysis is broadened to further smooth out the fluctuation of the aggregated wind farm power by using energy storage devices and smart grid technologies. Finally, the analytical results reveal that the proposed methodology allows for extended periods of energy delivery when wind speeds are low or not blowing.

KEYWORDS: Capacity factor, energy storage, power intermittency, penalty factor, smart grid, wind turbine

1 INTRODUCTION

Weather patterns are changing over a long period of time due to climate change, which is now obvious. Although these changes could be considered natural, human actions have been the primary cause

of climate change, mostly as a result of the burning of fossil fuels, which produces greenhouse gas emissions [1]. Global environmental deterioration and climate change are accelerated by the use of fossil fuels, specifically natural gas, crude oil, and coal, which are the major contributors to CO₂ emissions. For example, the escalating occurrence of thick smog-cloud over many major cities of the world for several months each year (e.g., in China [2]), rising healthcare costs because of carcinogenic emissions, devastating droughts, and floods [3] have become grave threats to the welfare and economic development of countries all over the world. As a result, governments have adopted new regulatory policies in response to the Paris Agreement's approval in 2015 and the Kyoto Protocol's predecessors in 2005, which raised awareness of the need to reduce CO₂ emissions and advance various low-carbon generation technologies [4].

These are the key drivers underlying the change of electric power generation from fossil fuels to clean energy sources such as wind, solar, and hydropower plants. Due to their advanced technology and environmental friendliness, renewable energy resources promise to make a significant contribution to power generation and the final energy user [5]. The wind is one of the most advantageous renewable energy sources, and it has garnered significant global attention as a result of increased investment in different wind turbine sizes, capacities, and technologies. This is mainly because the maximum power capacity of a single turbine can reach multi-megawatt levels, implying that installing this technology for power generation requires much smaller installation expenditures and lands compared to other smaller-scale renewable technologies when deployed on grid scales [6].

By the end of 2011, the total global wind capacity was 238.351 GW, with the United States leading the way in terms of installed capacity of 46.919 GW [7]. Wind power can now meet at least 20% of total consumer demand in countries such as Germany and Denmark. Spain is the second most populous country in Europe, with a total capacity of 27.089 GW of wind turbines installed. The country trails behind Germany with 62.81 GW and ahead of France with 17.382 GW [8]. As strong winds sweep across the country's mountains and plains, the Spanish government is providing substantial economic support for investment in wind energy technology [9]. As a result, the country's present wind turbine producers and wind farm owners, such as Gamesa Eólica which is the world's second-largest turbine manufacturer, Iberdrola which is the world's largest wind farm owner and operator), and Acciona Energa, have risen to the forefront of the worldwide wind energy industries which is the greatest wind farm builder and developer in the world). However, because wind energy is uncontrollable, rapid growth in wind power has had a growing impact on the power system's operational stability and security [10].

The active power generation of a typical wind turbine is a function of how fast the wind speed is, which varies continuously and introduces unfavorable uncertainties to the supplied power to the end user [11]. Power fluctuations can have a significant impact on system frequency, particularly when the wind farm is providing energy for islanded power systems or microgrids. Various forms of energy storage systems (i.e., battery energy storage systems (BESS)) can be operated in parallel to wind farms to mitigate the impact of wind uncertainties and variabilities [12]. The importance of energy storage comes into play when there is a surplus of power during high wind and low demand days and returns the power to the grid when there is a need for extra energy during a low wind or no wind and high demand days. The popularity and attention of projects based on variable renewable power and battery energy storage systems are rising globally [13]. In a competitive energy market, these projects are anticipated to serve as future electrical infrastructure for dispatchable power supply.

Other techniques, such as operating the wind farm below the maximum power point with a certain reserve [14] using pitch angle control technique [15] and integrating demand side units (DSU) using smart grid applications [16], are also used in the literature. However, curtailing the wind farm for the purpose of system reserve allocation has a considerable impact on the total investment cost [17]. Different from the literature, in the study we examined two strategies to manage both the surplus amount of wind power to avoid wind curtailment and to deal with power variations. The total number of wind turbines spread across multiple geographical locations to reduce power intermittency of the net power generation. It is important to note that the analysis makes use of real wind data from numerous sites in Spain that are publicly available for research. The research, however, is adaptable enough to be replicated for other regions, such as Iraq's Kurdistan Region, whenever reliable weather data becomes available. The main contribution of this paper is as follows:

1. A new technique for reducing wind power variability is proposed and tested using real wind data from genuine wind sites.
2. The variable wind power is combined with storage devices and smart grid technologies to enable long-term secure wind power generation.
3. The required energy storage capacity is evaluated with and without the integration of smart grids.

The rest of this paper is organized as follows: Section 2 presents the model of wind turbine power. Analysis and results are provided in Section 3. Finally, conclusions with remarkable future works are given in Section 4.

2 MODELING WIND POWER

In this section, the power curve of a typical wind turbine is graphically and mathematically investigated. A wind turbine's output power (P_{wind}) generation can be determined as per equation (1) [18]:

$$P_{wind} = 0.5 \rho A_r v^3 \quad (1)$$

where A_r denotes the rotor swept area in (m), ρ is the density of air in (kg/m³), v is the speed of the wind. The output power of a wind turbine is proportional to the cube of the wind speed, which implies that even a minor decrease in wind speed reduces the power generation dramatically. As an example, raising the average wind speed from 6 m/s to 7 m/s results in 60% more power and a 36% increase in annual energy production from the same turbine. This is schematically shown using the wind power curve in Figure 1 [19].

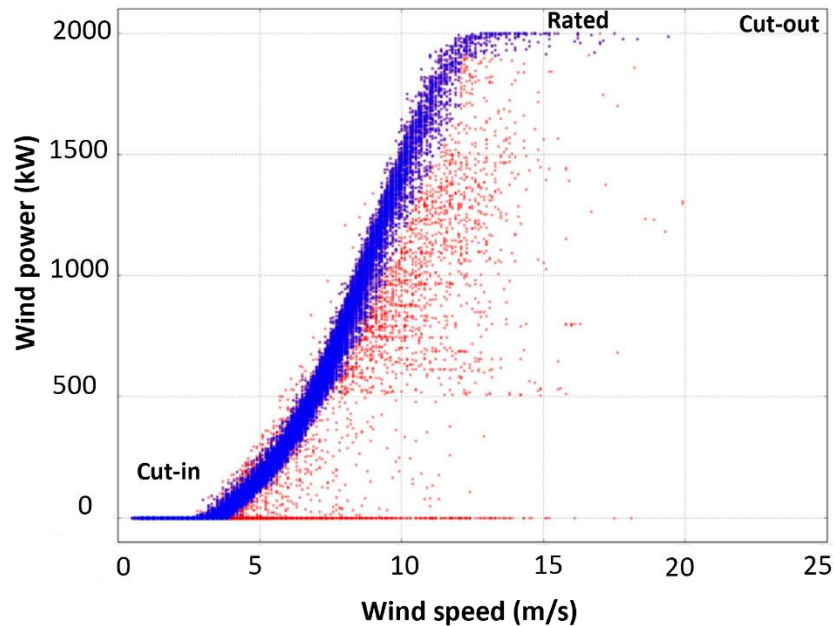


Figure 1: Characteristics of wind power generation versus speed of the wind for a typical wind turbine.

The active power output of a wind turbine can be classified based on the region of wind speed operation, as shown in Figure 1. The operational regions are basically divided into three main regions namely, cut-in, rated, and cut-out wind speed. This is derived using equation (2).

$$P_{wind} = \begin{cases} P_{rated} & \text{for } v_r < v \leq v_0 \\ P(v) & \text{for } v_i < v \leq v_r \\ 0 & \text{for } v_i > v > v_0 \end{cases} \quad (2)$$

where v_i , v_r , and v_0 represent the cut-in, rated, and cut-off wind speeds, respectively. Below the cut-in region, the wind turbine masses rotate extremely slowly, implying that the turbine will not be able to generate adequate active power and will not be required to remain in service. Above the cut-in regions, the wind turbine begins to generate power linearly with regard to wind speed until it reaches the maximum power point tracking, at which point the turbine generates the rated power. This remains constant until the cut-out region, where the wind speed exceeds 25m/s, requires the turbine to be disconnected from the national grid service.

Different wind speeds necessitate turbine operation at varied pitch angles, resulting in variable mechanical power (P_{mech}) and torque (T_w) characteristics that may be calculated using equations (3) and (4).

$$P_{mech} = P_{wind} C_p(\lambda, \beta) \quad (3)$$

$$T_w = 0.5 C_p(\lambda, \beta) \rho \pi R^3 V_w^2 / \lambda \quad (4)$$

where C_p denotes the turbine performance coefficient that is a factor of pitch angles and tip speed ratios, λ is the tip speed, β is the pitch angle of the blades, R refers to the radius of the turbine. The value of λ can be found from the turbine blade's peak speed to the speed of the wind, which is stated as (5).

$$\lambda = \omega R / v \quad (5)$$

The performance coefficient increases when the wind speed rises. Nevertheless, with a further increase in wind speed, the performance coefficient falls. As a result, wind turbines can be considered to self-regulate their output power by lowering their efficiency when the wind speed is high and increasing it when the wind speed is low. The performance coefficient of a wind turbine for different pitch angles is graphically depicted in Figure 2.

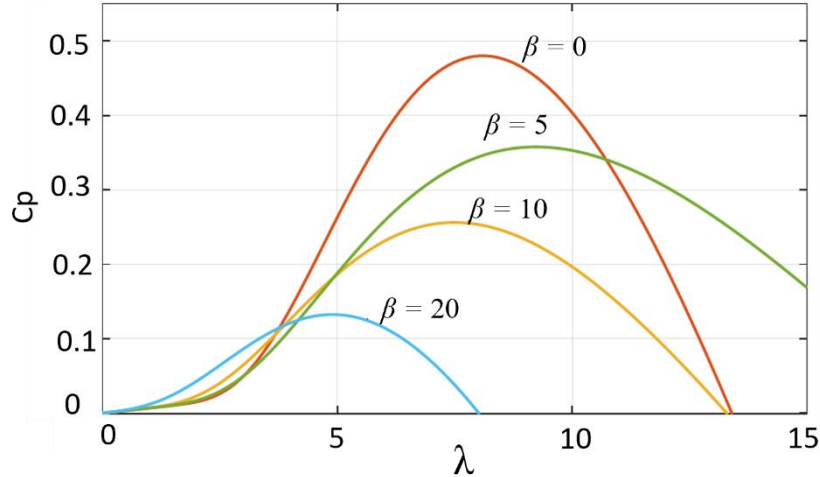


Figure 2: $C_p - \lambda$ characteristics of a wind turbine at different β [20].

3 ANALYSIS AND RESULTS

A relatively large wind farm is considered in this study. It is assumed that there are a significant number of turbines within a particular wind farm. The intermittency within the wind power is examined considering the target required output power is 200 MW. This precise output power is merely an assumption for the purposes of this analysis; alternatively, different active powers can be employed. A further assumption is made considering that the wind farm has a load factor of 30% [21]. This assumption implies renewable energy is weather dependent and does not produce power continuously similar to conventional power plants. Thus, the farm's output power generation varies greatly as a result of the load factor. Using these assumptions, two scenarios have been developed to visualize the proposed strategy.

3.1 First Scenario

To make this study more practical and applicable, the V90-3.0MW Vestas wind turbine is being explored. The tower height of this turbine is 80 meters, which allows the wind turbine to produce a peak output power of 3 MW when the wind speed reaches 15 m/s [22]. The cut-in speed is set to 3.5 m/s while the cut-out wind speed is set to 25 m/s. In this analysis, real wind speed data is collected for a site named Tarifa in Spain for a whole duration of one year. Tarifa is among the world's optimum locations for wind power generation. The meteorological wind data is measured at 10 meters in height [23]. The following three steps are then used to calculate the potential output power of each wind turbine:

Step 1: Wind speed at 80 meters high is calculated from data obtained at 10 meters to meet Vesta's standard turbine constraints. The wind measurements are simply multiplied by a factor of 119.27 percent, as established by the Danish Wind Industry Association wind data converter, as per equation (6) [24].

$$ws_{80} = ws_{10} \times 1.1927 \quad (6)$$

where ws_{80} denotes the wind speed at 80 m height in (m/s) and ws_{10} is the wind speed at 10 m height in (m/s). The wind speed measurement data for a complete duration of one year is shown in Figure 3.

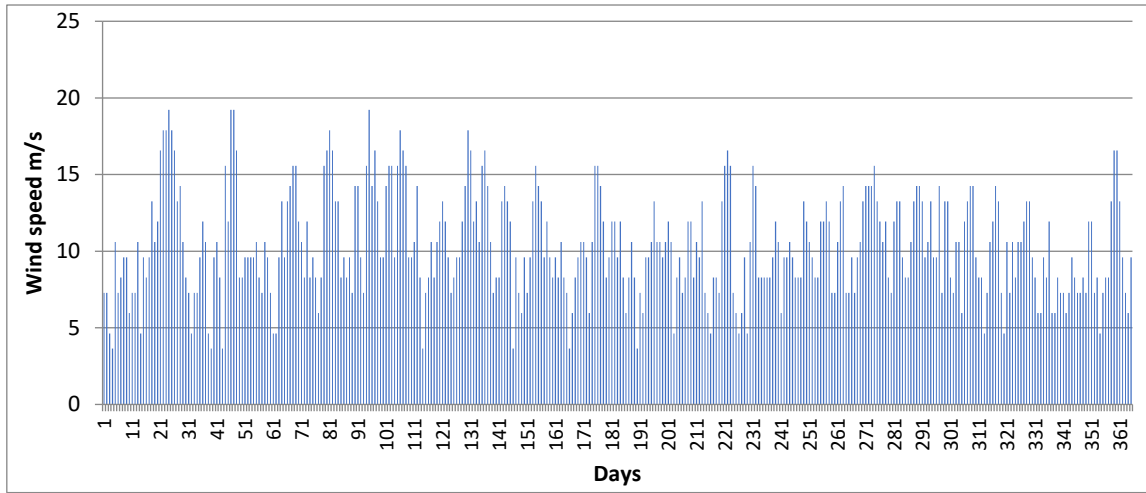


Figure 3: Tarifa meteorological wind speed data measured at 80 meters height.

Step 2: The manufacturer's power curve, shown in Figure 4, is used to calculate the power produced by turbines at each wind speed. The manufacturer data sheet does not include the actual mathematical equation for representing this graph. This implies that alternative ways to linearize this figure that can capture wind turbine active power generation as an alternative calculation method to the model's original equation are required. Thus, a linear interpolation is used between wind speeds of 5.5 m/s and 15 m/s to represent the area where wind power does not change linearly with wind speed. Other techniques can also be used as in [25]. However, we use the following simple linear interpolation computation method:

$$\frac{y - y_1}{x - x_1} = \frac{y_2 - y_1}{x_2 - x_1} \Rightarrow \frac{y - 0}{x - 5.5} = \frac{3 - 0}{15 - 5.5} \quad \text{Line equation: } y = 0.316x - 1.74 \quad (7)$$

where y is determined with respect to different x values. From (7) all the output power points that are in the range of 5.5 m/s to 15 m/s can be determined. It is also worth noting that with a further increase

in the wind speed above 15 m/s, the output power remains constant at 3 MW. Although this equation can not precisely reflect the output power of the turbine, it can produce satisfactory results. The same step can be repeated to determine the power generation for each turbine for a duration of one year using both equation (7) and the power curve displayed in Figure 4.

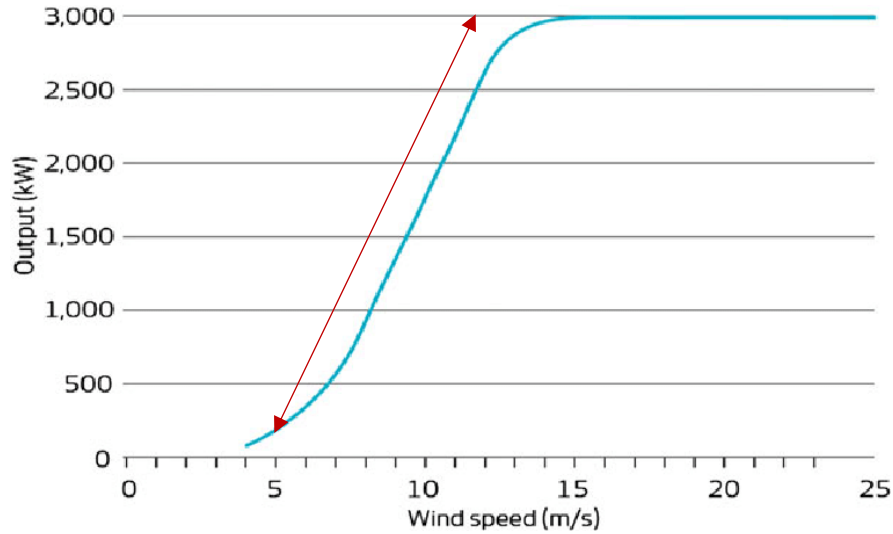


Figure 4: The standard power curve of Vestas V90-3.0MW turbine with a modified straight line.

Equation (7) now becomes (8) and can be used to determine wind turbine output power at different wind speed measurements up to 80 meters.

$$P_{out}(ws_{80}) = (ws_{80} \times 0.316) - 1.74 \quad (8)$$

As an example, the output power at 7.2 m/s per turbine can be calculated as below:

$$P_{out}(7.288 \text{ m/s}) = (7.288 \times 0.316) - 1.74 = 0.563 \text{ MW/Turbine}$$

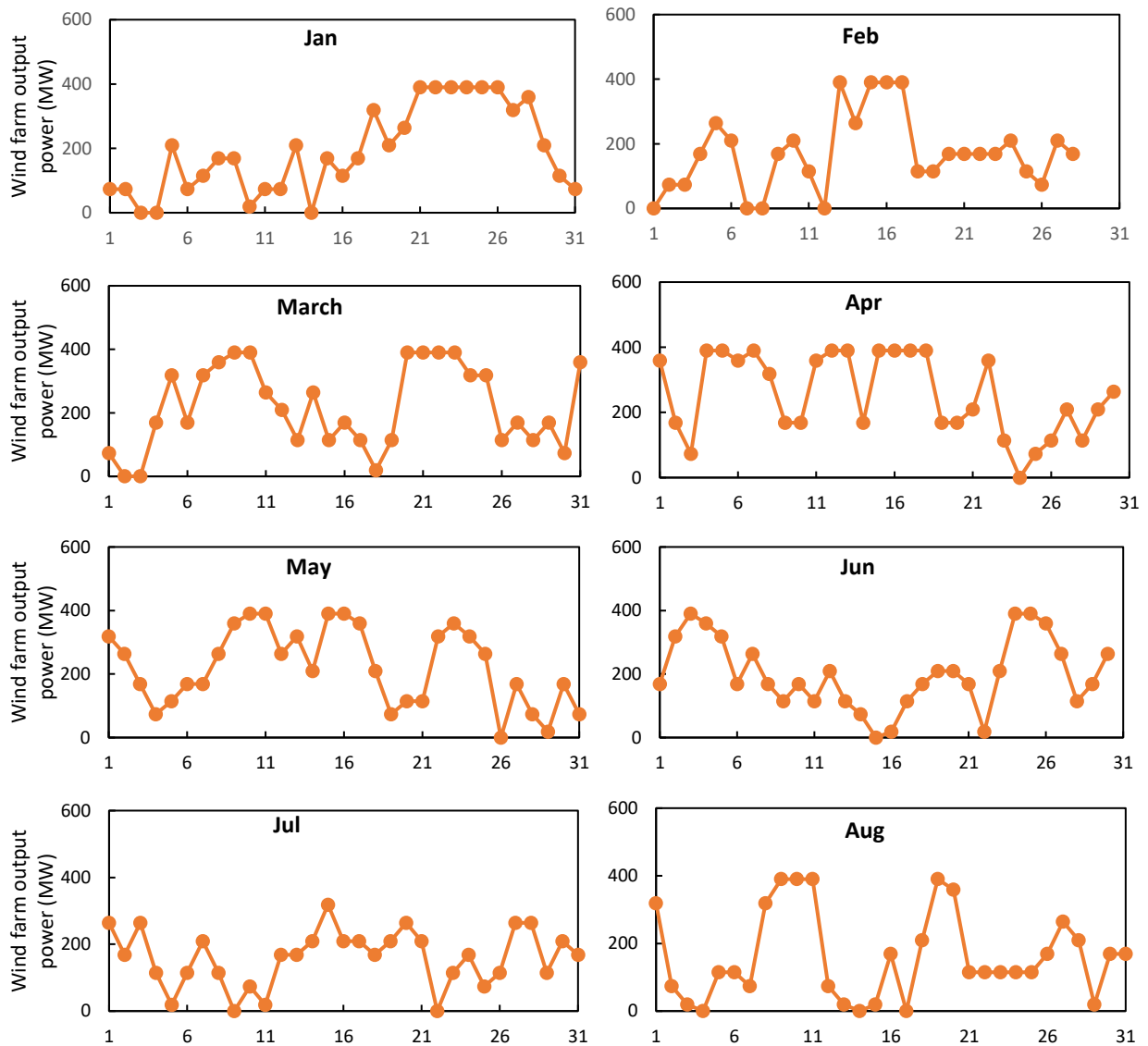
For N number of turbines in each site, the output power generation can be calculated using (9):

$$P_{Total} = P_{out} \times N \quad (9)$$

For instance, if 130 wind turbines are assumed to be in operation, at the wind speed of 7.2 m/s, the aggregated output power is as follows:

$$P_{Total}(130 \text{ turbines}) = 0.563 \times 130 = 73.48 \text{ MW}$$

This is one of the main steps of the analysis that is repeated 365 times to calculate the actual power generation of the wind farm over the time period of one year as shown in Figure 5. Each graph illustrates daily wind power generation for the proposed number of wind turbines for a complete duration of one month. It is important to note that wind power varies substantially, with some days having a cumulative power of more than 400 MW and others having wind power near to nil. For example, there are at least four days in January and February when wind power generation is nearly zero.



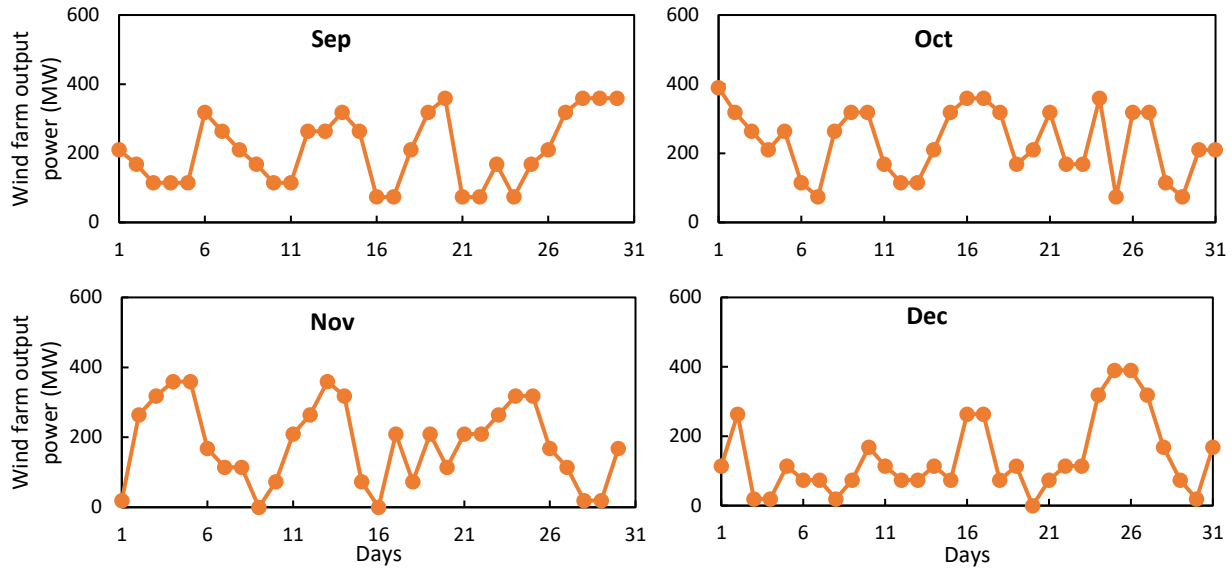


Figure 5: Daily power generation of 130 turbines over a course of one year (computed using equations (8) and (9)).

Furthermore, there is no clear comparison between these graphs over a year due to the variability of wind speed, which is weather dependent and changes so quickly. As can also be seen, claiming that wind power is high/low during winter/summer days is impossible. Interestingly, from January to April, there is a continuous wind wave that lasts for a number of days and results in continuous high power generation. For instance, from the 21st of January to the 28th, wind power remains constant at 400 MW while fluctuating the rest of the month. This means that such renewable power plants will have a daily surplus of energy that must be stored and used on days when wind production is extremely low. Another important observation from these graphs is that having low wind power for a few days in a row, like in December, necessitates large-scale energy storage devices to support renewable energy targets. Otherwise, conventional fossil-fuelled power plants must be restarted as an alternative solution to support power system demand, which will be both cost-effective and environmentally unfriendly. Other solutions include withdrawing active power from the network, as in smart demand response, or using demand response and grid-scale long-duration energy storage devices (i.e., hydrogen storage).

Turning now to mathematical calculations of the wind power generation and using the actual daily wind data from Figure 3, the accumulated wind power (P_{out}) generation of one turbine is calculated over a course of one year as follows:

$$P_{out} = 547.296 \text{ MW}$$

Given that each turbine's maximum ideal power generation is 3 MW, the total nameplate power might be calculated as follows:

$$P_{max} = 3 \text{ MW} \times 365 \text{ days} = 1095 \text{ MW}$$

where $P_{out}(ws_{80})$ is a real power generation for a turbine for a duration of one day for a wind turbine operating at 80 meters high, P_{Total} denotes the complete wind farm power generation in a day, N is the total number of turbines within a farm, P_{out} represents the real power of each turbine for a complete duration of one year, and P_{max} is peak power generation for a turbine within one year. Using the amount of power generated in a time period, versus the amount of power that could have been generated, the load factor (LF) can be derived as in (10).

$$L.F = P_{out}/P_{max} \quad (10)$$

$$L.F = 547.296 \text{ MW}/1095 \text{ MW} = 0.49 = 49\%$$

where $L.F$ is the load factor of a wind farm installed at the Tarifa site.

Step 3: The objective of this research is to examine, if possible, for a wind farm to produce a maximum power of 200 MW for a duration of 292 days in a year. In another word, the farm can be shut down for 73 days for maintenance and technical issues. A total of 130 turbines are assumed to be in operation in order to meet the objective of the 200 MW target. Equations (8) and (9) are used in this step to compute the wind farm's daily output power for a complete duration of one year.

The blue line in Figure 6 shows the power output of wind farms with 130 turbines, while the accumulated power and the 200 MW target are shown in brown and yellow, respectively. The accumulation power is the daily power generated by the farm minus 200 MW and can be maintained in the same way throughout the year. The plant's output power varies significantly, resulting in significant variance in accumulation over the course of a year. Similar power variations might be found even within a single day. As previously stated, the goal is to reduce wind power intermittency while also storing excess wind power during periods of strong wind power generation. This method will assist in maintaining a constant output power for a longer period of time. However, if the farm is turned off for 73 days for maintenance reasons, the accumulated electricity reaches $24 \text{ h} \times 3000 \text{ MW} = 72 \text{ MWh}$. However, storing this amount of energy can be a problem as it requires a significantly large scale of energy storage devices and that is not a practical option.

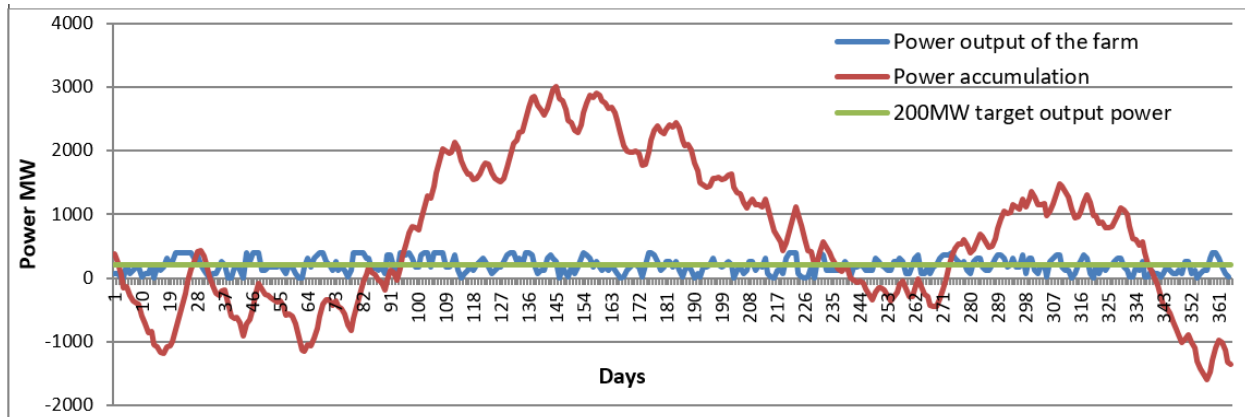


Figure 6: Combined daily output power for 130 wind turbines operating in parallel, daily accumulated power, and the target that we set for the plant.

3.2 Second Scenario

The distribution of wind turbines over multiple places rather than aggregating them in one region, as recommended in [26], is one way to reduce the plant's power intermittency. This strategy improves the total number of hours that the wind blows while decreasing the number of times when no energy is generated. It also minimizes the maximum instantaneous power generation, which reduces both the accumulated energy and the needed storage capacity. Figure 7 illustrates the preceding calculations performed to determine wind data at an altitude of 80 meters for two additional locations: Algeciras and Barbate, Spain. These two planned locations are close enough to the Tarifa site for the system operator to easily aggregate them as a single power plant. However, at different periods of the year, these locations experience varying wind speeds. To be more specific, Algeciras is located 11.26 kilometers northeast of Tarifa, while Barbate is 35 kilometers northwest. The wind turbines are distributed across these three locations as follows: 40 turbines in the Algeciras site, 50 turbines in the Tarifa site, and 40 turbines in the Barbante. Tarifa has the largest load factor of the three locations, which explains why there are more turbines there.

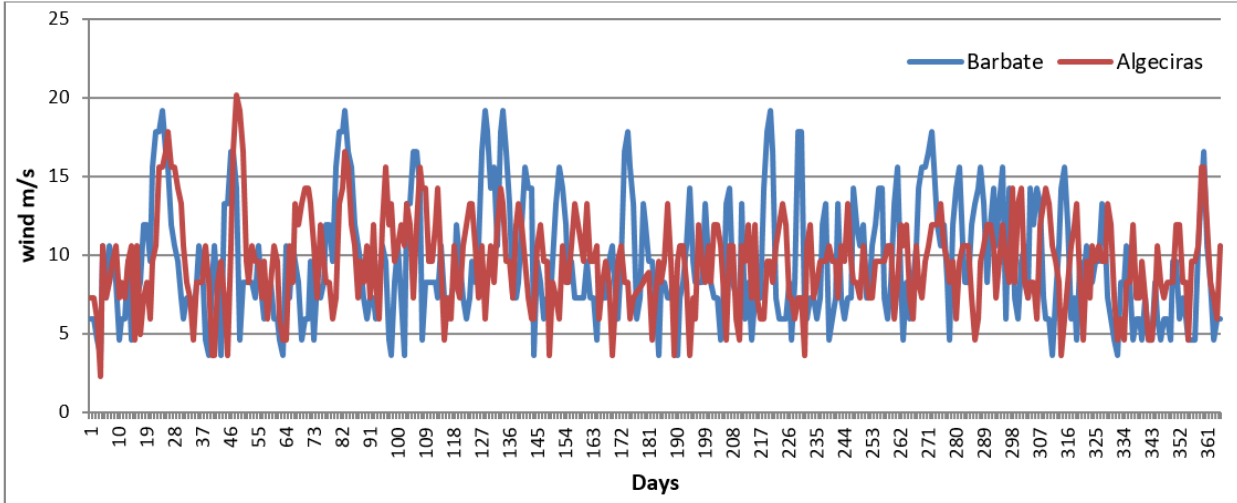


Figure 7: Wind data from Barbate and Algeciras at an altitude of 80 meters.

To compute daily power produced from each wind farm site, the previous equations and computational procedures are repeated. The output powers of the three locations are then aggregated and integrated into the power network as a large single provider. Figure 8 compares the output power of both scenarios for better clarification. It is apparent that the number of days when the plant is not producing has decreased dramatically meaning that the farm output power is now smoother as shown by the blue and red excel interpolation data lines.

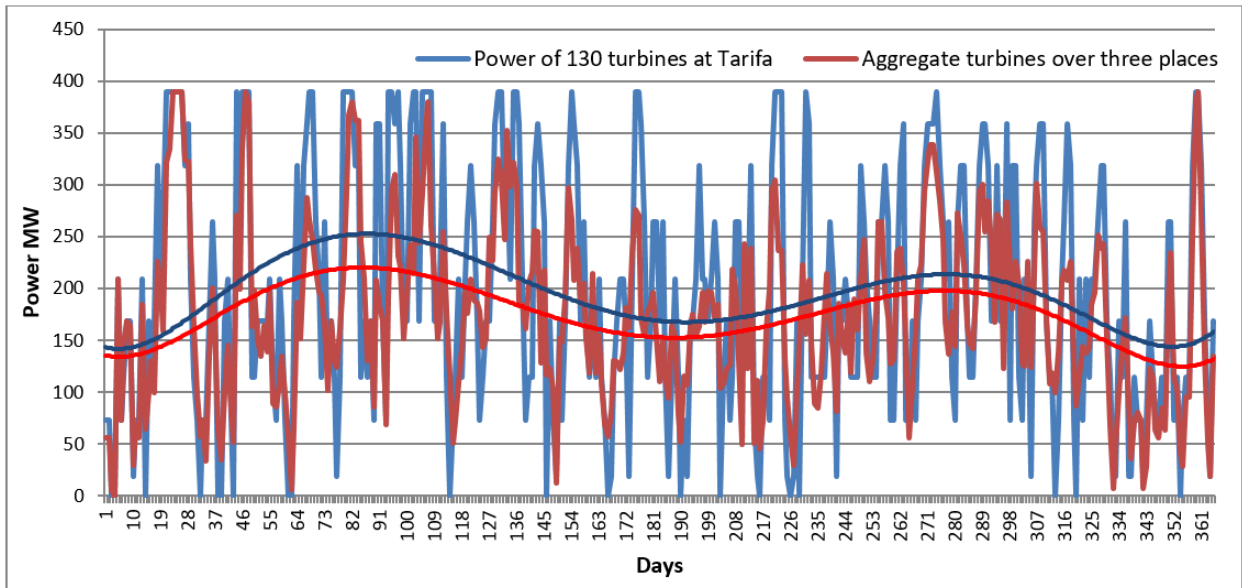


Figure 8: Wind farms output power for the aggregated wind turbines versus distributed over three locations, and the excel lines show how smoother is the average power.

The research is extended further to determine the required energy storage capacity if the accumulated energy is stored in an intelligent grid via DSU or without DSU. The size of storage systems must be kept as small as possible from an economic standpoint. To reduce storage capacity, this analysis proposes the integration of a smart grid and energy storage. The approximated storage capacity against the target energy for the proposed plant is shown in Figure 9. As observed, without the assumption of DSU, a maximum storage capacity of 70 GWh is required to store the extra energy over a year. Because the smart grid via DSU minimizes the wind farm's intermittency, the required energy storage capacity is reduced. As demonstrated in Figure 9, the accumulated energy curve does not contain any negative values, indicating that the wind farms can deliver 200 MW of active power for a full timeframe of 292 days without issue if integrated with storage or DSU.

To put things into perspective, this paragraph presents some factual information on global electric vehicle trends. By the end of 2020, there were 10 million electric cars on the road around the world [27], following a decade of rapid growth. Despite a global dip in car sales due to the pandemic, which saw global car sales drop by 16% in 2020, electric car registrations increased by 41%. Existing rules around the world point to considerable growth in the following decade: according to the Stated Policies Scenario, the total number of electric vehicles (excluding two/three-wheelers) would reach 145 million in 2030, representing 7% of the worldwide road vehicle fleet [27]. Higher power generation will be necessary in the European Union, for example, to meet the additional energy demand resulting from an 80 percent share of electric vehicles in 2050. Electric vehicles will account for roughly 4-5% of total electricity consumption in Europe by 2030, and 9.5% by 2050, up from 0.03% in 2014 [28]. Without a smart grid, total global energy storage requirements are expected to rise from 189 GW capacity to 305 GW by the end of 2050; however, this number is anticipated to decline to 122 GW from 260 GW if smart grids, electric vehicles, and demand response programs are integrated [29].

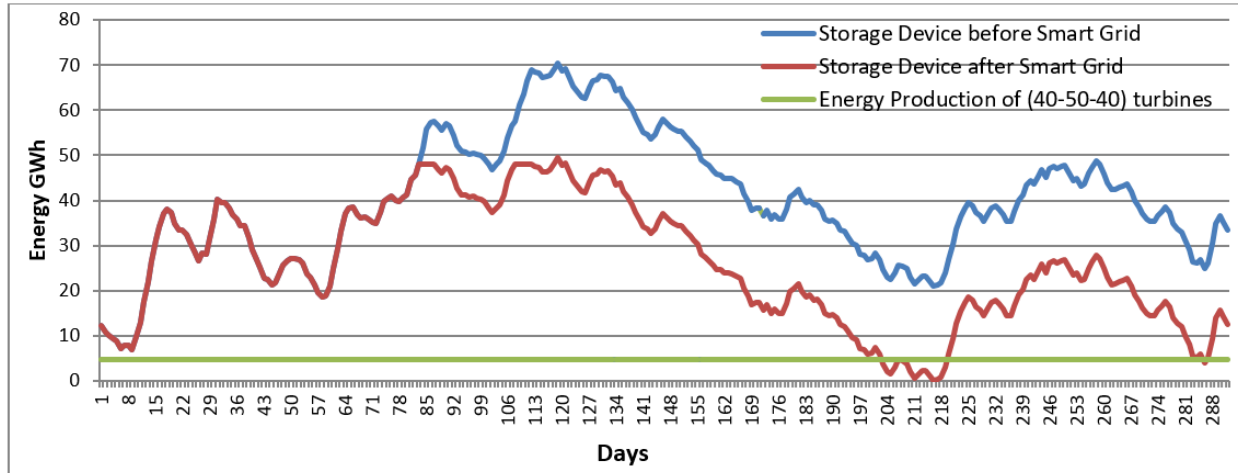


Figure 9: Required storage device to store the accumulated energy with and without a smart grid, and the required energy target.

Turning now to our model, one can expect that if the wind turbines are divided into three areas, they will be able to power a considerable number of electric vehicles under the scenario described previously. These cars can store surplus energy during periods of low demand and then release it during periods of high demand, similar to energy storage systems. As long as electric vehicles are accessible, this may be cheaper than turning off and curtailing wind power generation. As illustrated in Figure 9, the accumulative energy should not go below a negative value as wind power is assumed to attain the objective energy storage requirement within 292 days. The energy differential between the two lines can be used to calculate the predicted reduction in storage capacity owing to smart grid device energy consumption. As shown, a large amount of energy (i.e., 21.12 GWh) can be utilized by the smart grid without pushing the accumulative curve into the negative area of the graph. It is vital to remember that energy cannot be delivered to the smart grid before day 90, as this would cause the accumulative curve to collapse below the required target limits. Finally, there will be 12 GWh of excess power in the storage by the end of the year, which can be used at the start of the following year.

4 CONCLUSIONS

Renewable energy resources, particularly wind energy, have an enormous potential to play a significant role in the current electricity generation to meet the ever-increasing greenhouse gas emissions and demand escalation. However, one of the main issues with the deployment of grid-scale renewable energy sources is the output power's variability and intermittency, which significantly impact the power transmission to the end user. Fortunately, the continuous increase in renewable energy coincides with the development of smart

grids such as electric vehicles and battery energy storage systems. All these systems can be integrated to reduce renewable power uncertainties. This research examined a radically different technique for minimizing wind farm output power variability. As a case study, we used data from three wind-rich geographical sites in Spain. The proposed technique divides the number of contracted wind turbines over three locations rather than combining them in one. The analysis results showed that the power variability could be significantly reduced. However, it was discovered that the required storage could be quite enormous. Thus, smart DSU and energy storage devices are projected to consume extra energy to smooth the output power further. This increased wind farms' power variability and allowed them to store excess energy during high wind days and use it during low wind days.

REFERENCES

- [1] H. Qudrat-Ullah, "A review and analysis of renewable energy policies and CO₂ emissions of Pakistan," *Energy*, vol. 238, p. 121849, 2022, doi: 10.1016/j.energy.2021.121849.
- [2] I. Manisalidis, E. Stavropoulou, A. Stavropoulos, and E. Bezirtzoglou, "Environmental and Health Impacts of Air Pollution: A Review," *Front Public Heal.*, vol. 8, no. 14, 2020, doi: 10.3389/fpubh.2020.00014.
- [3] R. Ali, A. Kuriqi, and O. Kisi, "Human-environment natural disasters interconnection in China: A review," *Climate*, vol. 8, no. 4, pp. 1–28, 2020, doi: 10.3390/cli8040048.
- [4] D. Al Kez, "Power system dynamics with increasing distributed generation penetrations," Queen's University Belfast, PhD Thesis, 2022.
- [5] B. V. Mathiesen *et al.*, "Smart Energy Systems for coherent 100% renewable energy and transport solutions," *Appl. Energy*, vol. 145, pp. 139–154, 2015, doi: 10.1016/j.apenergy.2015.01.075.
- [6] and A. K. S. Prem Kumar Naik, Nirmal-Kumar C. Nair, "Impact of reduced inertia on transient stability of networks with asynchronous generation," *Int. Trans. Electr. ENERGY Syst.*, vol. 26, no. April 2015, pp. 175–191, 2015, doi: 10.1002/etep.2079.
- [7] S. Ahmed *et al.*, "Renewables Global Status Report," Paris, France, 2011. [Online]. Available: http://www.ren21.net/Portals/97/documents/GSR/REN21_GSR2011.pdf.
- [8] IRENA, "Renewable energy statistics 2021," International Renewable Energy Agency, Abu Dhabi, United Arab Emirates, 2021.
- [9] C. Edmunds, S. Martín-Martínez, J. Browell, E. Gómez-Lázaro, and S. Galloway, "On the participation of wind energy in response and reserve markets in Great Britain and Spain," *Renew. Sustain. Energy Rev.*, vol. 115, no. September, p. 109360, 2019, doi: 10.1016/j.rser.2019.109360.

- [10] B. Hoseinzadeh, F. Blaabjerg, Z. Chen, and R. Teodorescu, "Emergency wind power plant re-dispatching against transmission system cascading failures using reverse tracking of line power flow," *IET Gener. Transm. Distrib.*, vol. 14, no. 16, pp. 3241–3249, 2020, doi: 10.1049/iet-gtd.2019.1950.
- [11] N. Nguyen and J. Mitra, "An analysis of the effects and dependency of wind power penetration on system frequency regulation," *IEEE Trans. Sustain. Energy*, vol. 7, no. 1, pp. 354–363, 2016, doi: 10.1109/TSTE.2015.2496970.
- [12] X. Wu, X. Hu, X. Yin, and S. J. Moura, "Stochastic Optimal Energy Management of Smart Home With PEV Energy Storage," *IEEE Trans. Smart Grid*, vol. 9, no. 3, pp. 2065–2075, 2018, doi: 10.1109/TSG.2016.2606442.
- [13] P. Saini and L. Gidwani, "An investigation for battery energy storage system installation with renewable energy resources in distribution system by considering residential, commercial and industrial load models," *J. Energy Storage*, vol. 45, no. October 2021, p. 103493, 2022, doi: 10.1016/j.est.2021.103493.
- [14] H. Luo, Z. Hu, H. Zhang, and H. Chen, "Coordinated Active Power Control Strategy for Deloaded Wind Turbines to Improve Regulation Performance in AGC," *IEEE Trans. Power Syst.*, vol. 34, no. 1, pp. 98–108, 2019, doi: 10.1109/TPWRS.2018.2867232.
- [15] R. El Otmani and E. Otmani, "MPPT and pitch angle control for wind energy conversion system pitch angle control for wind energy conversion system pitch angle control for wind energy conversion system of selected sites in pitch angle control for wind energy conversion system MPPT and ," *IFAC Pap.*, vol. 55, no. 12, pp. 109–114, 2022, doi: 10.1016/j.ifacol.2022.07.296.
- [16] F. Conte, M. C. Di Vergagni, S. Massucco, F. Silvestro, E. Ciapessoni, and D. Cirio, "Synthetic Inertia and Primary Frequency Regulation Services by Domestic Thermal Loads," 2019, doi: 10.1109/EEEIC.2019.8783679.
- [17] G. Liu *et al.*, "Emergency Active Power Control Considering Power Reserve for Direct Driven Wind Power System Under Overspeed Power Shedding Operation," *Proc. - 2021 IEEE Sustain. Power Energy Conf. Energy Transit. Carbon Neutrality, iSPEC 2021*, pp. 3153–3158, 2021, doi: 10.1109/iSPEC53008.2021.9736000.
- [18] S. Shokrzadeh, M. Jafari Jozani, and E. Bibeau, "Wind turbine power curve modeling using advanced parametric and nonparametric methods," *IEEE Trans. Sustain. Energy*, vol. 5, no. 4, pp. 1262–1269, 2014, doi: 10.1109/TSTE.2014.2345059.
- [19] B. Manobel, F. Sehnke, J. A. Lazzús, I. Salfate, M. Felder, and S. Montecinos, "Wind turbine power

- curve modeling based on Gaussian Processes and Artificial Neural Networks,” *Renew. Energy*, vol. 125, pp. 1015–1020, 2018, doi: 10.1016/j.renene.2018.02.081.
- [20] C. I. Mart, J. D. Twizere-bakunda, D. Lundback-momp, S. Orts-grau, F. J. Gimeno-sales, and S. Segu, “Small Wind Turbine Emulator Based on Lambda-Cp Curves Obtained under Real Operating Conditions,” *Energies*, vol. 12, no. 13, 2019.
- [21] LuvSide GmbH, “Capacity factor of wind turbine: what influences electricity generation & what you should know about it,” 2020. <https://www.luvside.de/en/capacity-factor-wind-turbine/> (accessed Mar. 01, 2022).
- [22] VESTAS, “Proven technology to safeguard your investment - V90 3MW,” 2011. <https://pdf.archiexpo.com/pdf/vestas/v90-30-mw/88087-281441.html> (accessed Jan. 15, 2022).
- [23] Eltiempo, “Forecast History for Spain.” <http://en.eltiempo.es/tarifa.html?v=historico> (accessed Jun. 12, 2021).
- [24] Danish Wind Industry Association, “Wind Turbine Power Calculator,” 2003. http://drømstørre.dk/wp-content/wind/miller/windpower_web/en/tour/wres/pow/index.htm (accessed Sep. 08, 2021).
- [25] Y. Wang *et al.*, “Sparse heteroscedastic multiple spline regression models for wind turbine power curve modeling,” *IEEE Trans. Sustain. Energy*, vol. 12, no. 1, pp. 191–201, 2021, doi: 10.1109/TSTE.2020.2988683.
- [26] Y. Cai and F. Br, “Wind power potential and intermittency issues in the context of climate change,” *Energy Convers. Manag.*, vol. 240, p. 114276, 2021, doi: 10.1016/j.enconman.2021.114276.
- [27] International Energy Agency, “Global EV Outlook 2021 - Accelerating ambitions despite the pandemic,” Paris, France, 2021.
- [28] European Environment Agency, “Electric vehicles and the energy sector - impacts on Europe ’ s future emissions,” Copenhagen K, Denmark, 2021.
- [29] InternatIonal energy agency, “Modelling Load Shifting Using Electric Vehicles in a Smart Grid Environment,” Paris, France, 2010.